Insights into Imaging
EUROPEAN SOCIETY OF RADIOLOGY

ORIGINAL ARTICLE

Open Access

# Stiffness on shear wave elastography as a potential microenvironment biomarker for predicting tumor recurrence in HBV-related hepatocellular carcinoma

Xian Zhong[1], Haiyi Long[1], Lili Chen[2], Yuhua Xie[1], Yifan Shi[1], Jianyun Peng[1], Ruiying Zheng[1], Liya Su[1], Yu Duan[1], Xiaoyan Xie[1] and Manxia Lin[1*]

## Abstract

**Background** To explore the pathologic basis and prognostic value of tumor and liver stiffness measured pre-operatively by two-dimensional shear wave elastography (2D-SWE) in hepatitis B virus (HBV)-related hepatocellular carcinoma (HCC) patients who undergo hepatic resection.

**Methods** A total of 191 HBV-infected patients with solitary resectable HCC were prospectively enrolled. The stiffness of intratumoral tissue, peritumoral tissue, adjacent liver tissue, and distant liver tissue was evaluated by 2D-SWE. The correlations between stiffness and pathological characteristics were analyzed in 114 patients. The predictive value of stiffness for recurrence-free survival (RFS) was evaluated, and Cutoff Finder was used for determining optimal cut-off stiffness values. Cox proportional hazards analysis was used to identify independent predictors of RFS.

**Results** Pathologically, intratumoral stiffness was associated with stroma proportion and microvascular invasion (MVI) while peritumoral stiffness was associated with tumor size, capsule, and MVI. Adjacent liver stiffness was correlated with capsule and liver fibrosis stage while distant liver stiffness was correlated with liver fibrosis stage. Peritumoral stiffness, adjacent liver stiffness, and distant liver stiffness were all correlated to RFS (all $p < 0.05$). Higher peritumoral stiffness (> 49.4 kPa) (HR = 1.822, $p = 0.023$) and higher adjacent liver stiffness (> 24.1 kPa) (HR = 1.792, $p = 0.048$) were significant independent predictors of worse RFS, along with tumor size and MVI. The nomogram based on these variables showed a C-index of 0.77 for RFS prediction.

**Conclusions** Stiffness measured by 2D-SWE could be a tumor microenvironment and tumor invasiveness biomarker. Peritumoral stiffness and adjacent liver stiffness showed important values in predicting tumor recurrence after curative resection in HBV-related HCC.

**Clinical relevance statement** Tumor and liver stiffness measured by two-dimensional shear wave elastography serve as imaging biomarkers for predicting hepatocellular carcinoma recurrence, reflecting biological behavior and tumor microenvironment.

*Correspondence:
Manxia Lin
linmxia@mail.sysu.edu.cn
Full list of author information is available at the end of the article

**Key points**

- Stiffness measured by two-dimensional shear wave elastography is a useful biomarker of tumor microenvironment and invasiveness.
- Higher stiffness indicated more aggressive behavior of hepatocellular carcinoma.
- The study showed the prognostic value of peritumoral stiffness and adjacent liver stiffness for recurrence-free survival.
- The nomogram integrating peritumoral stiffness, adjacent liver stiffness, tumor size, and microvascular invasion showed a C-index of 0.77.

**Keywords** Hepatocellular carcinoma, Two-dimensional shear wave elastography, Microenvironment, Tumor recurrence, Stiffness

**Graphical Abstract**

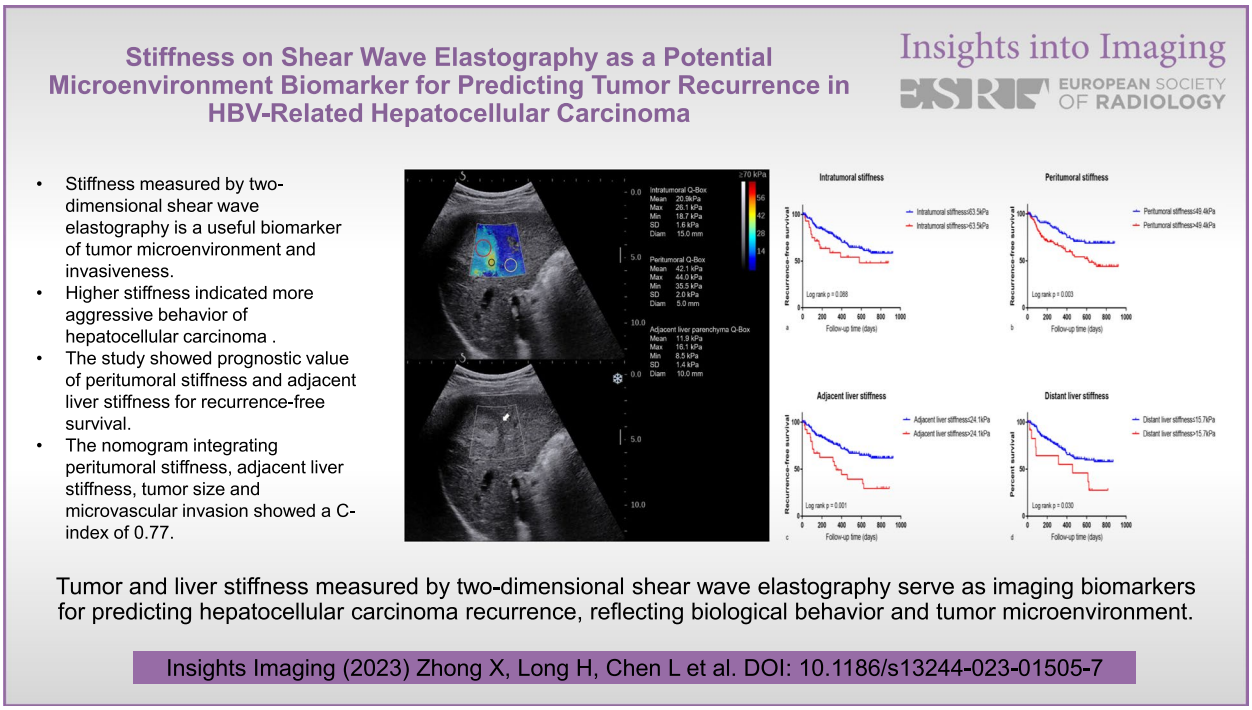


## Background

Hepatocellular carcinoma (HCC) is the fifth most common malignancy and the third leading cause of cancer-related death worldwide [1]. Surgical resection is the first-line therapy in patients with solitary tumors and well-preserved liver function. However, recurrence after surgical resection is common, with 5-year recurrence rates reaching 70% [2]. In addition to tumor size, tumor number, and liver function, the microenvironment and biologic behavior of tumors are also considered as important prognostic factors [3, 4].

The tissue stiffness reflects the mechanical properties and characterizes the complex interactions between tumor cells and extracellular matrix (ECM). The findings from various studies indicate that higher matrix stiffness promotes proliferation and chemotherapeutic resistance [5], upregulates VEGF expression [6], and enhances stemness [7] in HCC, which suggests the value of tissue stiffness to function as an integrative biomarker for HCC aggressiveness and prognosis [8]. Studies have demonstrated the value of tumor stiffness for predicting tumor recurrence following hepatic resection

[9–11], showing a positive correlation between higher tumor stiffness and increased recurrence rates. It was reported that higher matrix stiffness could trigger epithelial-mesenchymal transition in HCC and facilitate HCC invasion and metastasis, which suggested the role of tumor stiffness in characterizing tumor aggressiveness [5, 12]. Besides, liver stiffness was also reported to be an independent predictor of recurrence in HCC after surgical resection or radiofrequency ablation [13–17]. The liver stiffness, mainly related to the degree of liver fibrosis, has been proved to be involved in both carcinogenesis and progression of HCC [18–20]. Therefore, both tumor stiffness and liver stiffness could serve as comprehensive biomarkers for evaluating the tumor microenvironment, offering the possibility of being a prognostic marker for HCC recurrence.

The two-dimensional shear wave elastography (2D-SWE) technique is an ultrasound-based technique for real-time visualization of soft tissue's viscoelastic properties by measuring the speed of shear waves generated using acoustic radiation force [21]. The performance for assessment of diffuse liver disease by 2D-SWE has been confirmed [21, 22].

Several studies have also demonstrated the utility of 2D-SWE for the evaluation of tissue stiffness and for diagnosis or prognosis of focal liver lesions (FLLs) [23–26], and for characterizing tumor microenvironment and revealing the behavior of tumor-stroma interactions in HCC [27]. It may provide important tumor biologic, pathological, and ultimately prognostic information for HCC patients. Previous studies have reported the prognostic value of stiffness measured by magnetic resonance elastography, transient elastography, or acoustic radiation force impulse elastography for HCC recurrence [9–11, 13–17]. However, it remains unclear whether tumor stiffness and liver stiffness measured by 2D-SWE can also be used as prognostic markers for HCC recurrence after curative treatment. Furthermore, the pathological basis of the stiffness in HCC is also unknown.

Therefore, the hypothesis of this study is that tumor stiffness and liver stiffness measured by 2D-SWE can reflect the biological behavior and tumor microenvironment, thus serving as an imaging biomarker for predicting the prognosis of HCC. This study aimed to assess the pathological basis of tumor and liver stiffness and to evaluate the potential utility of tissue stiffness measured by 2D-SWE for predicting the recurrence of hepatitis B virus (HBV)-related HCC patients after hepatic resection, with a focus on combining tumor stiffness and liver stiffness for prediction.

## Materials and methods

### Patients

This prospective study was approved by the ethics committee of the First Affiliated Hospital of Sun Yat-Sen University. Written informed consents were obtained from all patients before enrollment. HBV-infected patients with solitary HCC who underwent surgical resection from February 2019 to February 2021 were consecutively included in this study according to the inclusion and exclusion criteria. The diagnosis of HCC before surgery was based on the American Association for the Study of Liver Diseases (AASLD) guideline [2]. Inclusion criteria included the following: (1) patients aged 18–80 years; (2) patients with solitary resectable HCC; (3) performance status Eastern Cooperative Oncology Group score 0–1. Exclusion criteria included the following: (1) poor quality of 2D-SWE image data (e.g., the elastography color map was less than 75% filled); (2) the lesions received local or systematic anti-tumor therapies before 2D-SWE examination or surgery; (3) Pathological confirmation of non-HCC lesions. Figure 1 shows the patient recruitment process.

### Ultrasound data acquisition

Both conventional ultrasound and 2D-SWE examinations were performed within one week before surgery. All examinations were performed by an Aixplorer Ultrasound system (SuperSonic Imagine, France) equipped with an SC6-1 convex probe by a radiologist with more than 10 years of ultrasound experience and more than 3 years of experience in liver 2D-SWE examination (M.X.L.).

After overnight fasting for at least 8 hours, the patient was placed in the supine position with the right arm in maximal abduction. 2D-SWE examination was performed for both tumor and liver according to the European Federation of Societies for Ultrasound in Medicine and Biology (EFSUMB) guideline [21]. For 2D-SWE examination of the tumor and adjacent liver, a B-mode ultrasound scan was first performed to determine the maximum cross-section of the tumor and adjacent liver parenchyma of at least 1cm. Then the ultrasound mode was switched to elasticity imaging mode. A 2D-SWE window of 4 cm × 3 cm was placed at a depth of 1–8 cm beneath the liver capsule and the scale was 70 kPa [28]. For tumors < 3 cm, the 2D-SWE window overlaid the tumor and adjacent liver parenchyma of at least 1.0 cm [29]. For tumors ≥ 3 cm, the 2D-SWE window overlaid a part of the tumor and adjacent liver parenchyma of at least 1.0 cm. The patients were asked to hold their breath for several seconds during quiet breathing and

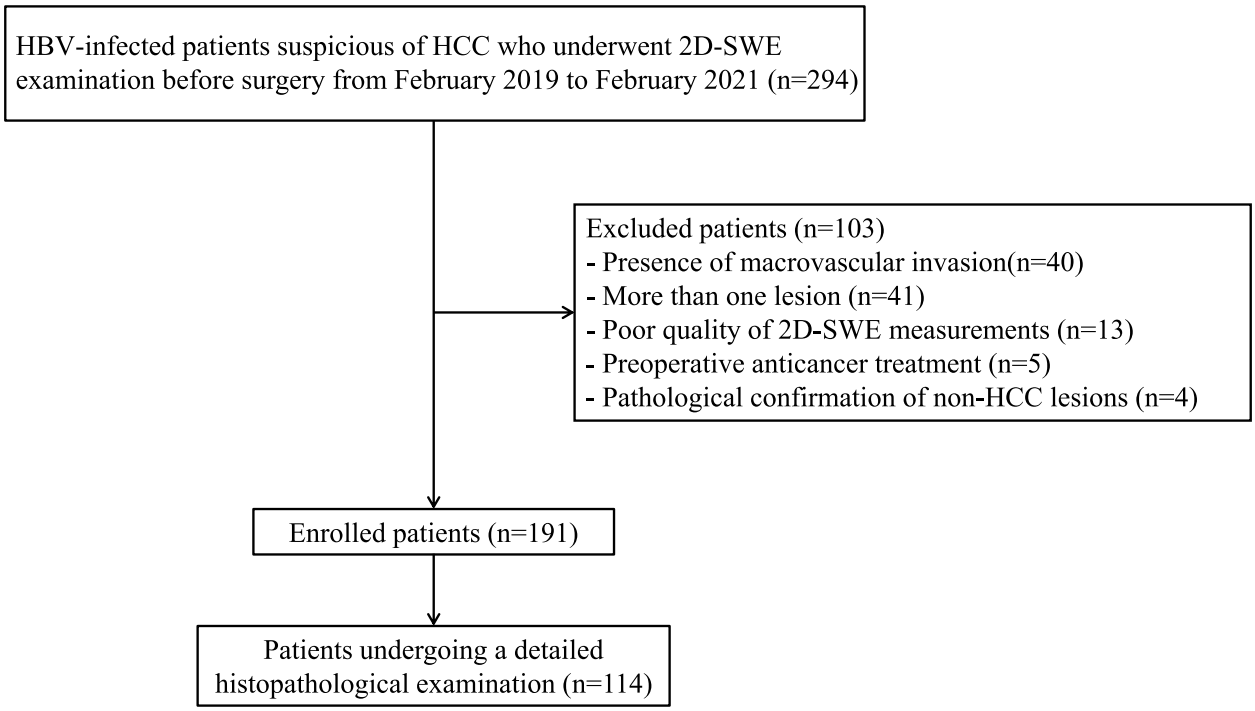


**Fig. 1** Flow chart of the enrolled patients in our study

five sequential images were obtained when the color map filled more than 75% of the 2D-SWE window and the signal stabilized for a few seconds [30]. For 2D-SWE examination of distant liver tissue, a B-mode ultrasound scan was first performed to locate a well-visualized liver area free of large vessels (diameter > 3 mm) and at least 5 cm away from the lesion margin. Areas in the right anterior lobe of the liver were preferred if available. Then the ultrasound mode was switched to elasticity imaging mode with the scale of 40 kPa. A 2D-SWE window of 4 cm × 3 cm was placed at a depth of 1.5–2 cm beneath the liver capsule. Patients were asked to hold their breath for a few seconds to obtain five sequential images once the elastography signal became stable and the color filling in the sampling frame reached 75%. The median and interquartile range (IQR) of five sequential acquisitions (in kilopascals) was calculated. An IQR/median < 30% was considered successful.

### Image analysis

The B-mode ultrasound and 2D-SWE images were analyzed by one radiologist (X.Z.) with more than 5 years of experience in ultrasound, who was unaware of the pathological results. Evaluations of B-mode ultrasound images were performed from the PACS system. The 2D-SWE image analysis was performed on the machine using the built-in ROI (Q-box) whose size and position were adjustable.

Evaluations of tumor B-mode ultrasound images included tumor size, shape, boundary, and presence of hypoechoic halo. Evaluations of 2D-SWE images included quantitative stiffness of both intratumoral and peritumoral tissue, as well as adjacent liver parenchyma and distant liver parenchyma. An intratumoral Q-box was placed inside the tumor to cover the tumor area as much as possible for intratumoral stiffness [26]. A peritumoral Q-box of about 5 mm was placed in the tumor border with the highest stiffness [31, 32]. An adjacent liver parenchyma Q-box of about 1cm was placed in adjacent liver parenchyma [26] (Fig. 2a). A distant liver parenchyma Q-box of about 2 cm was placed in distant liver parenchyma (Fig. 2b). The mean values (Emean) of Young's modulus in these four areas were recorded. The median values of Emean in five sequential images were used for further analysis.

### Clinical data collection and pathological examination

Preoperative patient characteristics and laboratory data were collected within one week ahead of surgery. Due to the unavailability of some pathological specimens, the pathological specimens of 114 patients from February 2019 to January 2020 were reviewed by a pathologist (L.L.C.) with more than 10 years of experience in HCC

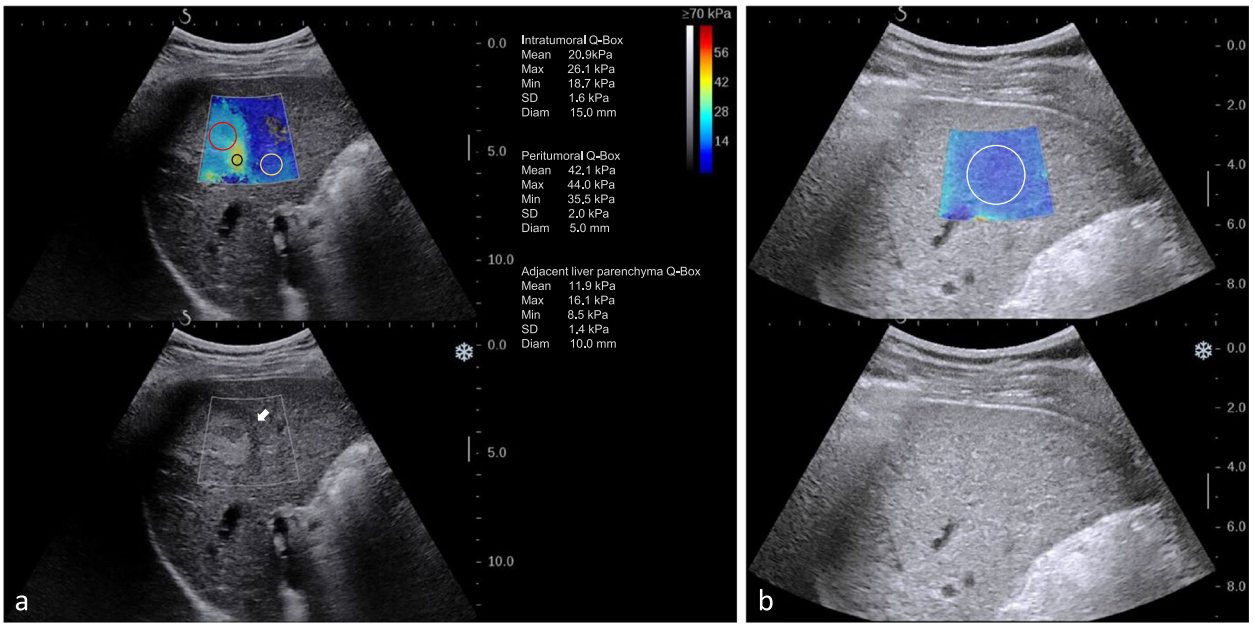


**Fig. 2** Elasticity measurement of 2D-SWE images. **a** Regions of interest (ROI) for measurement of the stiffness of intratumoral tissues (red ROI), peritumoral tissues (black ROI), and adjacent liver parenchyma (yellow ROI). **b** ROI for distant liver parenchyma (white ROI)

pathology, without knowing the patient's clinical data and ultrasound results. The specimens were sampled according to the 7-point baseline sampling protocol [33]. Information about Edmondson-Steiner grade, proportion of stroma, the presence and proportion of tumor necrosis, the presence of tumor capsule, degree of peritumoral lymphocytic reaction, microvascular invasion (MVI) of HCC, and grade of liver fibrosis were evaluated using a microscope on 4-μm paraffin-embedded histological sections with hematoxylin and eosin staining. The presence of cirrhosis was defined as S4 according to the Scheuer liver fibrosis staging system by pathological examination [34]. Definitions of the other pathological characteristics can be found in the Supplementary material.

### Follow-up

Patients were consistently followed up after liver resection at intervals of 3 to 6 months based on serum alpha-fetoprotein and imaging examination (contrast-enhanced computed tomography or contrast-enhanced magnetic resonance imaging). All patients were under anti-viral treatment after resection. All patients were followed up until September 2021. The mean period of follow-up was 14.2 ± 9.2 months (range 1.5–30.7 months). Recurrence-free survival (RFS) was calculated from the date of surgical resection to the tumor recurrence (local recurrence, new intrahepatic tumor, vascular invasion, or distant organ metastasis). RFS was censored at the date of death or of the last follow-up visit for recurrence-free patients.

### Statistical analysis

Statistical analyses were performed by using SPSS, version 20.0, and R4.1.2. The Student's *t*-test or the Mann-Whitney test, as appropriate, was used to compare continuous variables in recurrence and non-recurrence groups. The $\chi^2$ test was used to compare categorical variables. The elasticity values of different pathological manifestations were compared by using the Mann-Whitney test. An online tool Cutoff Finder was used to determine the optimal cut-off elasticity values for predicting RFS [35]. The elasticity values were dichotomized based on the optimal cut-off values. Univariable and multivariable analyses were performed to determine the significant clinical, ultrasound, and pathological factors for RFS prediction. The survival curves were generated using the Kaplan–Meier method and the log-rank test was applied to compare the differences between groups. After the univariable Cox proportional hazards model was applied to each variable, the variables with a $p$ value less than 0.05 entered multivariate analysis to identify independent predictors for RFS based on stepwise Cox proportional

**Table 1** Clinical and ultrasound characteristics of patients included in this study

| Characteristic | All patients ($n = 191$) | Non-recurrence group ($n = 125$) | Recurrence group ($n = 66$) | *p* value |
|---|---|---|---|---|
| Age (year)[a] | 55.0 (47.0–64.0) | 55.0 (47.5–64.0) | 55.0 (46.5–62.5) | 0.346 |
| Sex | | | | 0.354 |
| Male | 173 (90.6) | 115 (92.0) | 58 (87.9) | |
| Female | 18 (9.4) | 10 (8.0) | 8 (12.1) | |
| Tumor size (cm)[a] | 5.3 (3.6–7.8) | 4.7 (3.3–6.5) | 7.7 (5.0–10.5) | < 0.001 |
| BCLC stage | | | | 0.205 |
| Very early stage (0) | 3 (1.6) | 3 (2.4) | 0 (0.0) | |
| Early stage (A) | 188 (98.4) | 122 (97.6) | 66 (100.0) | |
| Child-Pugh class | | | | 0.949 |
| A | 185 (96.9) | 121 (96.8) | 64 (97.0) | |
| B | 6 (3.1) | 4 (3.2) | 2 (3.0) | |
| Edmondson-Steiner grade | | | | 0.099 |
| Grade I–II | 88 (46.1) | 63 (50.4) | 25 (37.9) | |
| Grade III–IV | 103 (53.9) | 62 (49.6) | 41 (62.1) | |
| Microvascular invasion | | | | < 0.001 |
| Absent | 110 (57.6) | 84 (67.2) | 26 (39.4) | |
| Present | 81 (42.4) | 41 (32.8) | 40 (60.6) | |
| Cirrhosis of background liver | | | | 0.310 |
| Absent | 139 (72.8) | 88 (70.4) | 51 (77.3) | |
| Present | 52 (27.2) | 79 (29.6) | 15 (22.7) | |
| AFP | | | | 0.006 |
| ≤ 20 U/L | 90 (47.1) | 68 (54.4) | 22 (33.3) | |
| > 20 U/L | 101 (52.9) | 57 (45.6) | 44 (66.7) | |
| TBIL | | | | 0.816 |
| ≤ 17.1 μmol/L | 138 (72.3) | 91 (72.8) | 47 (71.2) | |
| > 17.1 μmol/L | 53 (27.7) | 34 (27.2) | 19 (28.8) | |
| ALB | | | | 0.244 |
| < 35 g/L | 164 (85.9) | 110 (88.0) | 54 (81.8) | |
| ≥ 35 g/L | 27 (14.1) | 15 (12.0) | 12 (18.2) | |
| ALT | | | | 0.751 |
| ≤ 40 U/L | 133 (69.6) | 88 (70.4) | 45 (68.2) | |
| > 40 U/L | 58 (30.4) | 37 (29.6) | 21 (31.8) | |
| AST | | | | 0.005 |
| ≤ 40 U/L | 116 (60.7) | 85 (68.0) | 31 (47.0) | |
| > 40 U/L | 75 (39.3) | 40 (32.0) | 35 (53.0) | |
| GGT | | | | 0.007 |
| ≤ 50 U/L | 92 (48.2) | 69 (55.2) | 23 (34.8) | |
| > 50 U/L | 99 (51.8) | 56 (44.8) | 43 (65.2) | |
| HBV-DNA | | | | 0.178 |
| ≤ 100 IU/mL | 88 (46.1) | 62 (49.6) | 26 (39.4) | |
| > 100 IU/mL | 103 (53.9) | 63 (50.4) | 40 (60.6) | |
| Intratumoral stiffness (kPa) [a] | 32.1 (20.6–49.8) | 31.5 (10.5–48.1) | 35.7 (23.1–53.1) | 0.179 |
| Peritumoral stiffness (kPa) [a] | 48.3 (30.4–62.7) | 43.8 (28.2–60.5) | 51.9 (39.4–66.3) | 0.020 |
| Adjacent liver stiffness (kPa) [a] | 12.5 (9.5–18.7) | 12.7 (9.5–18.3) | 12.2 (9.7–21.4) | 0.600 |
| Distant liver stiffness (kPa) [a] | 8.8 (7.0–11.4) | 8.5 (6.8–10.6) | 9.2 (7.3–12.0) | 0.123 |

*AFP*, alpha-fetoprotein; *TBIL*, total bilirubin; *ALB*, albumin; *ALT*, alanine aminotransferase; *AST*, aspartate transaminase; *GGT*, gamma-glutamyl transferase; *HBV*, hepatitis B virus

Unless otherwise indicated, data are shown as number of patients, with the percentage in parentheses

[a] Data are shown as median (interquartile range)

hazards regression. Schoenfeld residuals were used to check the proportional hazards assumption of the Cox proportional hazards model and a stepwise Cox regression was used to prevent multicollinearity. A nomogram was constructed based on independent predictors. The discrimination performance was quantified by concordance index (C-index) and area under the receiver operating characteristic curve (AUC) at 0.5 years, 1 year, and 2 years. The calibration performance was determined by calibration curve analysis. All statistical tests were two-tailed and a $p$ value < 0.05 was considered a statistically significant difference.

## Results

### Baseline characteristics

A total of 191 HBV-infected patients with single HCC who underwent surgical resection were prospectively enrolled in this study, including 173 males and 18 females with a median age of 55.0 (47.0–64.0) years (Fig. 1).

During the follow-up, HCC recurrence was observed in 66 (34.6%) patients. The baseline characteristics of the recurrence group, non-recurrence group, and all patients were summarized in Table 1. There were significant differences in tumor size ($p < 0.001$), presence of MVI ($p < 0.001$), AFP level ($p = 0.006$), AST level

**Table 2** Correlations between pathological characteristics and tissue stiffness

| Pathological characteristics | Intratumoral stiffness (kPa) | *p* | Peritumoral stiffness (kPa) | *p* | Adjacent liver stiffness (kPa) | *p* | Distant liver stiffness (kPa) | *p* |
|---|---|---|---|---|---|---|---|---|
| Tumor size | | 0.533 | | 0.014 | | 0.959 | | 0.607 |
| ≤ 5 cm | 33.9 (18.6–49.4) | | 40.7 (23.2–50.5) | | 11.3 (8.9–18.9) | | 8.8 (7.0–11.5) | |
| > 5 cm | 33.6 (24.6–49.9) | | 53.3 (33.9–64.6) | | 11.8 (9.0–18.0) | | 9.3 (7.6–10.8) | |
| Proportion of stroma | | 0.016 | | 0.165 | | 0.290 | | 0.754 |
| ≤ 20% | 30.9 (16.7–40.8) | | 43.3 (30.2–55.2) | | 12.9 (9.1–20.6) | | 9.2 (7.5–11.7) | |
| > 20% | 35.4 (26.5–54.2) | | 51.7 (28.0–66.5) | | 11.1 (8.7–17.4) | | 9.1 (7.2–10.8) | |
| Tumor necrosis | | 0.203 | | 0.230 | | 0.997 | | 0.288 |
| Absent | 27.9 (17.8–50.1) | | 44.9 (21.7–61.2) | | 12.5 (8.1–19.4) | | 9.1 (7.9–12.8) | |
| Present | 34.9 (25.6–49.8) | | 48.8 (30.2–64.7) | | 11.7 (9.2–18.0) | | 9.2 (7.2–10.6) | |
| Proportion of necrosis | | 0.158 | | 0.205 | | 0.454 | | 0.828 |
| < 20% | 32.9 (20.8–44.2) | | 44.7 (23.9–61.9) | | 12.0 (9.0–19.4) | | 8.5 (7.3–11.4) | |
| ≥ 20% | 34.5 (26.0–55.1) | | 51.7 (30.1–68.2) | | 11.0 (8.9–17.5) | | 9.4 (7.0–11.0) | |
| Edmondson-Steiner grade | | 0.376 | | 0.104 | | 0.833 | | 0.577 |
| Grade I–II | 30.7 (20.8–43.6) | | 44.3 (25.2–55.7) | | 12.1 (8.2–19.2) | | 9.1 (7.0–12.2) | |
| Grade III–IV | 34.5 (23.1–52.1) | | 51.1 (30.3–67.6) | | 11.1 (9.2–17.7) | | 9.3 (7.4–10.6) | |
| Tumor capsule | | 0.602 | | 0.004 | | 0.026 | | 0.497 |
| Absent | 35.3 (18.3–57.9) | | 30.4 (19.3–47.7) | | 9.5 (8.0–12.9) | | 8.7 (6.6–10.9) | |
| Present | 32.9 (23.6–46.5) | | 50.2 (32.1–63.9) | | 12.3 (9.3–19.4) | | 9.3 (7.5–11.5) | |
| Peritumoral lymphocytic reaction | | 0.542 | | 0.353 | | 0.605 | | 0.541 |
| Low | 31.3 (16.8–46.1) | | 43.8 (24.2–63.3) | | 11.9 (9.5–20.7) | | 8.5 (6.9–11.4) | |
| Moderate | 32.4 (25.4–49.0) | | 50.6 (39.7–66.5) | | 11.9 (9.5–17.5) | | 9.3 (7.9–10.7) | |
| High | 38.2 (22.4–54.0) | | 44.9 (25.3–61.0) | | 10.3 (8.1–18.7) | | 11.4 (6.6–19.4) | |
| Microvascular invasion | | 0.015 | | 0.021 | | 0.121 | | 0.219 |
| Absent | 30.6 (18.3–43.2) | | 40.5 (23.6–61.9) | | 10.9 (8.6–17.5) | | 8.5 (7.2–10.5) | |
| Present | 39.9 (30.4–53.4) | | 52.7 (40.3–63.9) | | 13.4 (9.3–10.9) | | 10.2 (7.9–11.8) | |
| Cirrhosis of background liver | | 0.777 | | 0.050 | | 0.036 | | 0.002 |
| Absent | 33.7 (21.2–48.9) | | 43.6 (25.2–48.8) | | 10.9 (8.2–17.3) | | 8.7 (6.9–10.5) | |
| Present | 33.4 (25.6–52.6) | | 54.1 (40.3–52.7) | | 13.7 (10.5–19.5) | | 11.4 (8.2–12.9) | |

(See figure on next page.)

**Fig. 3** Correlations between pathological characteristics and tissue stiffness. **a**, **b** Differences in intratumoral stiffness between patients with different subgroups of stroma proportion and status of microvascular invasion. **c**–**e** Differences in peritumoral stiffness between patients with different subgroups of tumor size, tumor capsule, and status of microvascular invasion. **f**, **g** Differences in adjacent liver stiffness between patients with different subgroups of tumor capsule and cirrhosis status. **h** Differences in distant liver stiffness between patients with different cirrhosis status

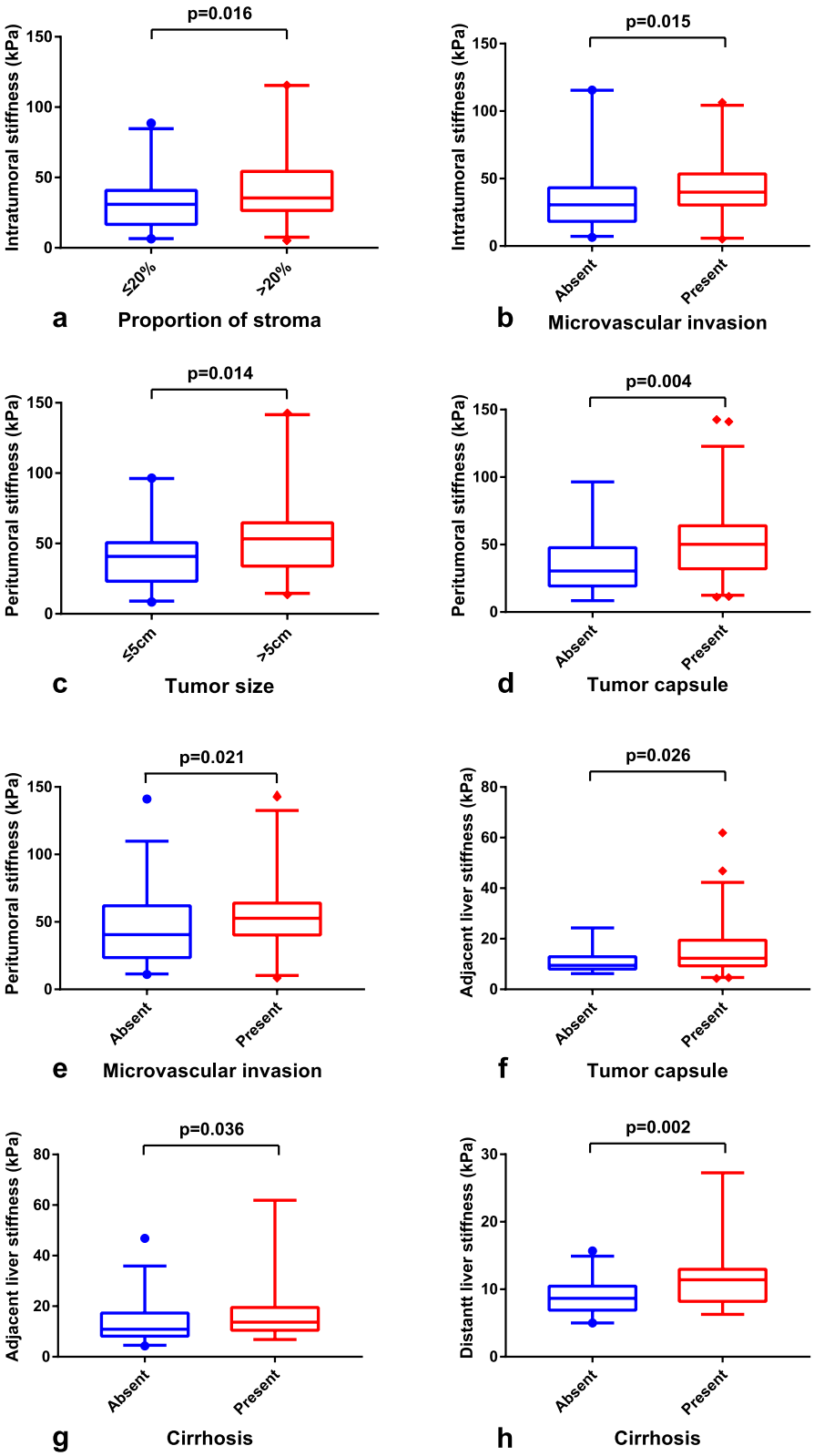


**Fig. 3** (See legend on previous page.)

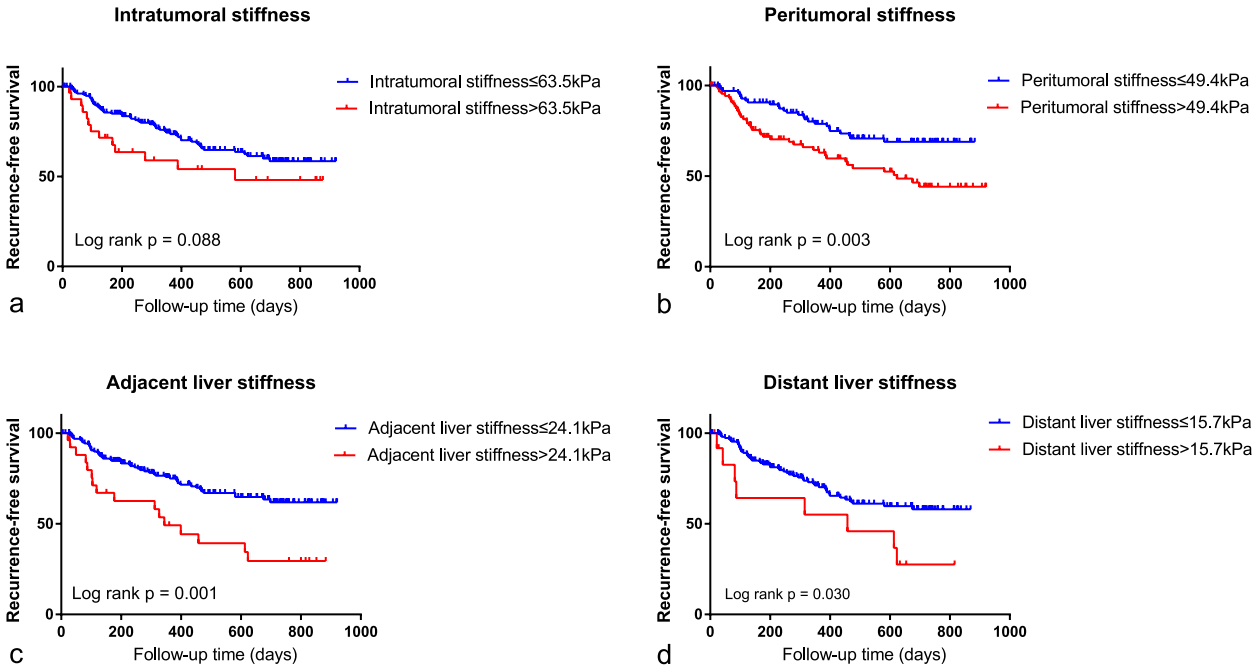


**Fig. 4** Correlations between recurrence-free survival and tissue stiffness. **a** Recurrence-free survival curves stratified by intratumoral stiffness. **b** Recurrence-free survival curves stratified by peritumoral stiffness. **c** Recurrence-free survival curves stratified by adjacent liver stiffness. **d** Recurrence-free survival curves stratified by distant liver stiffness

($p$ = 0.005), GGT level ($p$ = 0.007), and peritumoral stiffness ($p$ = 0.020) between the recurrence group and non-recurrence group.

### Pathological basis of intratumoral, peritumoral, adjacent liver and distant liver elasticity

Comparisons of intratumoral stiffness, peritumoral stiffness, adjacent liver stiffness, and distant liver stiffness between different pathological characteristics in 114 patients were shown in Table 2 and Fig. 3. Intratumoral stiffness was higher in tumors with the proportion of stroma of > 20% compared with tumors with the proportion of stroma of ≤ 20% ($p$ = 0.016) and in tumors with MVI compared with those without MVI ($p$ = 0.015). Peritumoral stiffness was higher in tumors with larger tumor size (> 5 cm, $p$ = 0.014), presence of tumor capsule ($p$ = 0.004), and presence of MVI ($p$ = 0.021). Adjacent liver stiffness was significantly correlated with the presence of a tumor capsule ($p$ = 0.026) and cirrhosis of the background liver ($p$ = 0.036). While distant liver stiffness was significantly correlated with cirrhosis of background liver ($p$ = 0.002).

### Quantitative 2D-SWE features and recurrence

The optimal cut-off values of intratumoral stiffness, peritumoral stiffness, adjacent liver stiffness, and distant liver stiffness for predicting RFS were 63.5 kPa, 49.4 kPa, 24.1 kPa, and 15.7 kPa, respectively. Based on these cut-off values, patients were dichotomized into two groups and RFS was compared between the two groups. Kaplan–Meier survival analysis showed that RFS was significantly shorter in patients with higher peritumoral stiffness ($p$ = 0.003), adjacent liver stiffness ($p$ = 0.001), and distant liver stiffness ($p$ = 0.030) compared with lower ones (Fig. 4). However, there was no significant difference in RFS between patients with high intratumoral stiffness and low intratumoral stiffness ($p$ = 0.088).

### Univariable and multivariable Cox proportional hazards analyses for predictors for RFS

Univariable Cox proportional hazards analysis showed that peritumoral stiffness (HR = 2.104; 95% CI, 1.283–3.450; $p$ = 0.003), adjacent liver stiffness (HR = 2.509; 95% CI, 1.428–4.408; $p$ = 0.001), and distant liver stiffness (HR = 1.249; 95% CI, 1.065–4.751; $p$ = 0.034) were associated with RFS (Table 3). With regard to clinical, histological and B-mode ultrasound features, tumor size (HR = 1.205; 95% CI, 1.149–1.264; $p$ < 0.001), AFP level (HR = 2.078; 95% CI, 1.245–3.369; $p$ = 0.005), AST level (HR = 2.119; 95% CI, 1.306–3.439; $p$ = 0.002), GGT level (HR = 1.931; 95% CI, 1.164–3.206; $p$ = 0.011), MVI (HR = 2.901; 95% CI, 1.768–4.762; $p$ < 0.001), and Edmondson-Steiner grade (HR=1.686; 95% CI, 1.024–2.775; $p$ = 0.040) were associated with RFS (Table 3).

Multivariable Cox proportional hazards analysis showed that larger tumor size (adjusted HR=1.190; 95% CI, 1.125–1.258; $p < 0.001$), MVI (adjusted HR = 1.764; 95% CI, 1.031–3.018; $p = 0.038$), higher peritumoral stiffness (> 49.4 kPa) (adjusted HR = 1.822; 95% CI, 1.088–3.051; $p = 0.023$), and higher adjacent liver stiffness (> 24.1 kPa) (adjusted HR = 1.792; 95% CI, 1.005–3.196; $p = 0.048$) were significant independent predictors of worse RFS (Table 3). The forest plot in Fig. 5 showed the results of multivariable Cox proportional hazards analysis.

### Development and validation of the nomogram for predicting RFS

The final nomogram integrated tumor size, MVI, peritumoral stiffness, and adjacent liver stiffness (Fig. 6a). The C-index of the nomogram was 0.77 (0.713–0.827). Receiver operating characteristic (ROC) curves to predict 0.5-, 1-, and 2-year recurrence-free RFS were shown in Fig. 6b with AUCs of 0.847, 0.818, and 0.777, respectively. The calibration curve showed good calibration for the nomogram to predict 0.5-, 1-, and 2-year recurrence-free RFS (Fig. 6c).

## Discussion

In this study, the pathological basis and prognostic implications of tumor stiffness and liver stiffness measured by 2D-SWE were explored in HBV-related HCC patients with solitary lesions and treated with surgical resection. The results indicated the important role of stiffness as an imaging biomarker of the tumor microenvironment and tumor invasiveness. Four stiffness characteristics, including intratumoral stiffness, peritumoral stiffness, adjacent liver stiffness, and distant liver stiffness, were analyzed in the current study. In HCC, higher values of the four stiffness were correlated with more aggressive metrics, such as higher proportion of stroma, presence of MVI, and larger tumor size. For the prognostic implications, peritumoral stiffness and adjacent liver stiffness were shown more valuable than intratumoral stiffness and distant liver stiffness in predicting tumor recurrence. Higher peritumoral stiffness (> 49.4 kPa) and higher adjacent liver stiffness (> 24.1 kPa) were independent risk factors for recurrence following hepatic resection in HBV-related HCC, along with traditional predictors such as larger tumor size and presence of MVI.

In this study, increased intratumor stiffness and peritumoral stiffness were shown to be associated with higher stroma proportion and the presence of tumor capsule, which were consistent with other studies showing that increased stiffness is mainly correlated with ECM remodeling and the deposition of ECM components [36, 37]. Many tumors are characterized by ECM deposition, remodeling, and cross-linking that drive

**Table 3** Univariate and multivariate analysis for predictors of RFS after HCC hepatectomy

| Variables | Univariate analysis | | Multivariate analysis | |
|---|---|---|---|---|
| | HR (95% CI) | *p* value | HR (95% CI) | *p* value |
| Sex, female vs. male | 1.410 (0.693–2.955) | 0.363 | | |
| Age, years | 0.989 (0.968–1.010) | 0.290 | | |
| Tumor size, cm | 1.205 (1.149–1.264) | < 0.001 | 1.190 (1.125–1.258) | < 0.001 |
| AFP, > 20 U/L vs. ≤ 20 U/L | 2.078 (1.245–3.369) | 0.005 | | |
| TBIL, > 17.1 μmol/L vs. ≤ 17.1 μmol/L | 1.049 (0.616–1.788) | 0.860 | | |
| ALB, < 35 g/L vs. ≥ 35 g/L | 1.623 (0.868–3.036) | 0.129 | | |
| ALT, > 40 U/L vs. ≤ 40 U/L | 1.094 (0.652–1.837) | 0.733 | | |
| AST, > 40 U/L vs. ≤ 40 U/L | 2.119 (1.306–3.439) | 0.002 | | |
| GGT, > 50 U/L vs. ≤ 50 g/L | 1.931 (1.164–3.206) | 0.011 | | |
| HBV-DNA, > 100 IU/mL vs. ≤ 100 IU/mL | 1.454 (0.887–2.383) | 0.137 | | |
| Cirrhosis, present vs. absent | 0.686 (0.385–1.222) | 0.201 | | |
| MVI, present vs. absent | 2.901 (1.768–4.762) | < 0.001 | 1.764 (1.031–3.018) | 0.038 |
| Edmondson-Steiner grade, III–IV vs. I–II | 1.686 (1.024–2.775) | 0.040 | | |
| Shape, irregular vs. regular | 1.655 (0.986–2.780) | 0.057 | | |
| Boundary, unclear vs. clear | 1.243 (0.665–2.325) | 0.496 | | |
| Halo, present vs. absent | 0.950 (0.575–1.569) | 0.840 | | |
| Intratumoral stiffness, > 63.5 kPa vs. ≤ 63.5 kPa | 1.685 (0.918–3.093) | 0.092 | | |
| Peritumoral stiffness, > 49.4 kPa vs. ≤ 49.4 kPa | 2.104 (1.283–3.450) | 0.003 | 1.822 (1.088–3.051) | 0.023 |
| Adjacent liver stiffness, > 24.1 kPa vs. ≤ 24.1 kPa | 2.509 (1.428–4.408) | 0.001 | 1.792 (1.005–3.196) | 0.048 |
| Distant liver stiffness, > 15.7 kPa vs. ≤ 15.7 kPa | 1.249 (1.065–4.751) | 0.034 | | |

*AFP*, alpha-fetoprotein; *TBIL*, total bilirubin; *ALB*, albumin; *ALT*, alanine aminotransferase; *AST*, aspartate transaminase; *GGT*, gamma-glutamyl transferase; *HBV*, hepatitis B virus; *MVI*, microvascular invasion

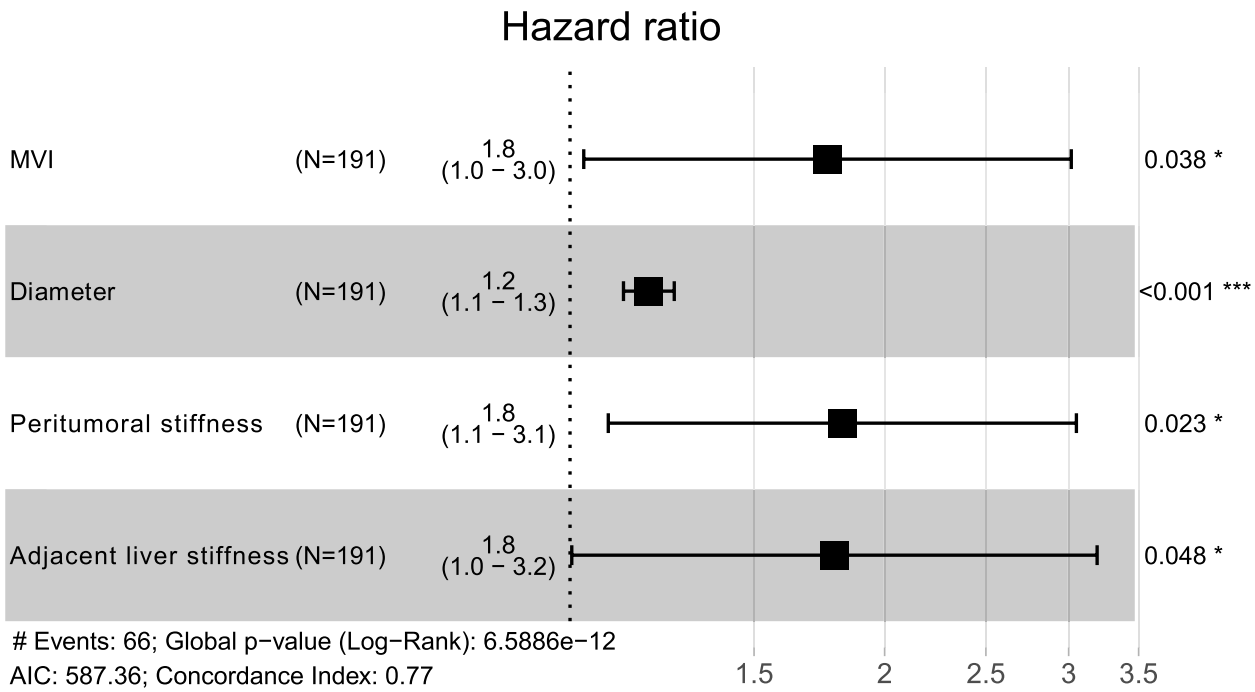


**Fig. 5** Forest plot of independent predictors of recurrence-free survival after hepatocellular carcinoma resection

fibrosis to stiffen the stroma and promote malignancy [38]. Increased stiffness can, in turn, promote numerous cellular functions that promote tumor progression and invasiveness [37]. This study also showed that intratumoral and peritumoral stiffness were correlated with the presence of MVI, a histopathologic evidence of tumor aggressiveness, which was consistent with present studies [39, 40]. These results indicated that tumor stiffness could be used as a potential biomarker to assess changes in the tumor microenvironment and tumor aggressiveness. The prognostic value of tumor stiffness was confirmed in the current study for predicting HCC recurrence after curative resection. Besides, intratumoral and peritumoral stiffness were assessed separately in this study, which was different from previous studies that integrated intratumoral and peritumoral stiffness [9–11]. Peritumoral stiffness was identified as an independent predictor of tumor recurrence. Several studies have confirmed that cancer-associated fibroblasts (CAFs), mainly located at the tumor marginal zone, enhance the production and reorganization of the ECM and lead to a mechanically stiff microenvironment [41]. Higher stiffness could promote tumor cell proliferation and invasion [5, 8]. However, our results did not show an independent prognostic value of intratumoral stiffness. This may be because that intratumoral stiffness could also be influenced by many other factors besides the stroma proportion, like the density of cancer cells and the presence of necrotic areas [36].

The microenvironment in which HCC develops also exerts a major influence on tumor development and growth [42]. This study showed that adjacent liver stiffness and distant liver stiffness were correlated with capsule status and liver fibrosis stage. Liver fibrosis is associated with an increased risk of malignancy [43]. Several studies have confirmed the role of liver stiffness in predicting HCC recurrence [13–16]. Our results showed that higher distant liver stiffness (> 15.7 kPa) was correlated with shorter RFS ($p = 0.030$), but no significant difference was found in cirrhosis presence between patients with and without recurrence. The inconsistency may be due to different cutoff values because liver stiffness ≥11 kPa is considered as cirrhosis in SuperSonic Imaging [44]. In this study, the results showed that although higher adjacent liver stiffness and higher distant liver stiffness were both related to a higher probability of recurrence, adjacent liver stiffness was shown to be an independent predictor of HCC recurrence. Periphery zones of tumor tissues are representative of tumor heterogeneity in that they are rich in highly invasive cells, which are susceptible to the formation of MVI and satellite nodules and impact postoperative recurrence [33]. Evidence also indicated that the infiltration of activated hepatic stellate cells (HSC) within adjacent liver tissues was closely associated with a poor prognosis of HCC after curative resection [45]. Activated HSCs may lead to a stiff environment and promote tumor cell dissemination [46], which may

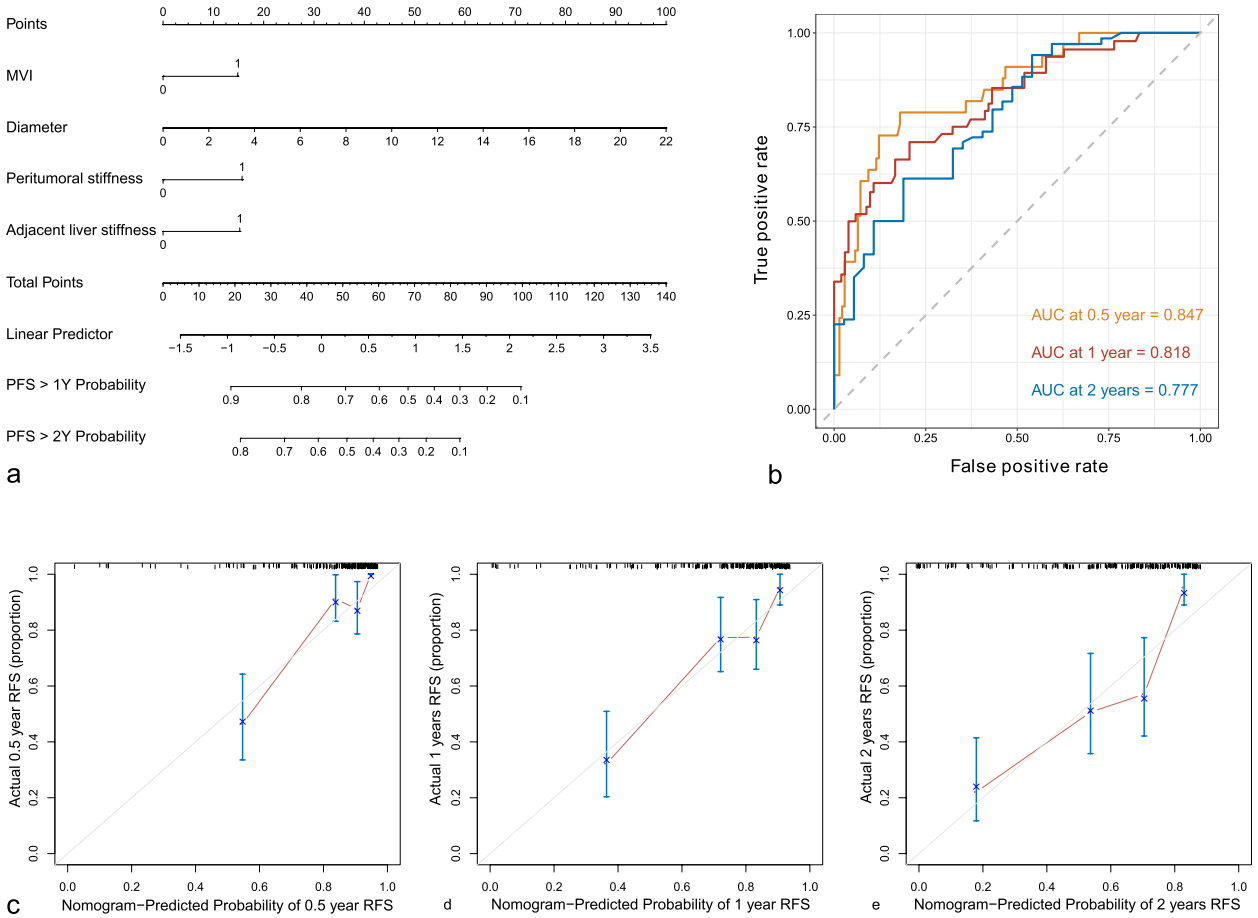


**Fig. 6** Performance of the nomogram. **a** Nomogram for predicting the recurrence-free survival in patients with hepatocellular carcinoma. **b** Receiver operating characteristic curves of the nomogram to predict 0.5-, 1-, and 2-year recurrence-free survival. **c**–**e** Calibration plots of the nomogram to predict 0.5-, 1-, and 2-year recurrence-free survival

explain the prognostic value of adjacent liver tissue stiffness. The reason that distant liver stiffness did not show independent prognostic value may be that most patients were treated with antiviral therapy postoperatively, which attenuated the effect of distant liver stiffness on recurrence prediction.

A nomogram integrating tumor size, MVI, peritumoral stiffness, and adjacent liver stiffness was established with a C-index of 0.77 for RFS prediction, showing satisfactory discrimination and calibration performance. The nomogram may help stratify the risk of recurrence and improve individualized treatments and personalized surveillance strategies.

There were some limitations in this study. Firstly, there may be heterogeneity in HCC tissue while only the maximum section of the lesion was assessed. Secondly, the maximum detection depth of 2D-SWE is limited [21], but tumor elastography can still be obtained for most enrolled lesions through scanning in multiple orientations. Thirdly, quantitative elasticity measurements were acquired by a single radiologist, the generalization of the findings needs further investigation. Although the 2D-SWE approach showed high reproducibility [47], inter and intraobserver variability may affect both data acquisition and interpretation. Fourthly, only patients with hepatitis B virus-related HCC were included, so the prognostic value of the tumor stiffness and liver stiffness in other causes of underlying liver diseases and other types of liver cancer needs further study. Fifthly, this is a single-center study, and the results should be confirmed by further studies at multiple centers with larger samples.

## Conclusions

In conclusion, stiffness measured by 2D-SWE could be a useful imaging biomarker of the tumor microenvironment and tumor invasiveness in HBV-related HCC, with higher stiffness indicating more aggressive behavior. Peritumoral stiffness and adjacent liver stiffness showed important values in predicting tumor recurrence after curative resection in HBV-related HCC.

**Abbreviations**

| | |
|---|---|
| 2D-SWE | Two-dimensional shear wave elastography |
| AUC | Area under the receiver operating characteristic curve |
| ECM | Extracellular matrix |
| Emean | Mean elastic modulus |
| HBV | Hepatitis B virus |
| HCC | Hepatocellular carcinoma |
| MVI | Microvascular invasion |
| RFS | Recurrence-free survival |

## Supplementary Information

The online version contains supplementary material available at https://doi.org/10.1186/s13244-023-01505-7.

**Additional file 1.**

**Authors' contributions**

XZ: conceptualization, data curation, investigation, methodology, software, validation, writing — original draft, writing — review and editing. HL: data curation, writing — original draft, writing — review and editing. LC: data curation, writing — original draft, writing — review and editing. YX: data curation, writing — original draft. YS: data curation. JP: data curation. RZ: data curation. LS: data curation. YD: data curation. XX: conceptualization, investigation, project administration, resources, supervision, writing — review and editing. ML: conceptualization, data curation, funding acquisition, project administration, supervision, writing — review and editing. All authors read and approved the final manuscript.

**Funding**

This study has received funding by the National Natural Science Foundation of China (No. 92059201 and 81901768).

**Availability of data and materials**

The datasets used and/or analyzed during the current study are available from the corresponding author on reasonable request.

## Declarations

**Ethics approval and consent to participate**

This prospective study was approved by the Ethics Committee of the First Affiliated Hospital of Sun Yat-sen University. Written informed consents were obtained from all patients in this study.

**Consent for publication**

Not applicable.

**Competing interests**

The authors declare that they have no competing interests.

**Author details**

[1]Department of Ultrasound, The First Affiliated Hospital of Sun Yat-Sen University, 58 Zhongshan Second Road, Guangzhou 510080, China. [2]Department of Pathology, The First Affiliated Hospital of Sun Yat-Sen University, 58 Zhongshan Second Road, Guangzhou 510080, China.

Received: 14 April 2023 Accepted: 16 August 2023
Published online: 12 September 2023

**References**

1. Sung H, Ferlay J, Siegel RL et al (2021) Global Cancer Statistics 2020: GLOBOCAN estimates of incidence and mortality worldwide for 36 cancers in 185 countries. CA Cancer J Clin 71:209–249
2. Marrero JA, Kulik LM, Sirlin CB et al (2018) Diagnosis, staging, and management of hepatocellular carcinoma: 2018 practice guidance by the American Association for the study of liver diseases. Hepatology 68:723–750
3. Sükei T, Palma E, Urbani L (2021) Interplay between cellular and non-cellular components of the tumour microenvironment in hepatocellular carcinoma. Cancers (Basel) 13(21):5586
4. Schulze K, Nault JC, Villanueva A (2016) Genetic profiling of hepatocellular carcinoma using next-generation sequencing. J Hepatol 65:1031–1042
5. Schrader J, Gordon-Walker TT, Aucott RL et al (2011) Matrix stiffness modulates proliferation, chemotherapeutic response, and dormancy in hepatocellular carcinoma cells. Hepatology 53:1192–1205
6. Dong Y, Xie X, Wang Z et al (2014) Increasing matrix stiffness upregulates vascular endothelial growth factor expression in hepatocellular carcinoma cells mediated by integrin β1. Biochem Biophys Res Commun 444:427–432
7. You Y, Zheng Q, Dong Y et al (2016) Matrix stiffness-mediated effects on stemness characteristics occurring in HCC cells. Oncotarget 7:32221–32231
8. Levental KR, Yu H, Kass L et al (2009) Matrix crosslinking forces tumor progression by enhancing integrin signaling. Cell 139:891–906
9. Park SJ, Yoon JH, Lee DH, Lim WH, Lee JM (2021) Tumor stiffness measurements on MR elastography for single nodular hepatocellular carcinomas can predict tumor recurrence after hepatic resection. J Magn Reson Imaging 53:587–596
10. Wang J, Shan Q, Liu Y et al (2019) 3D MR elastography of hepatocellular carcinomas as a potential biomarker for predicting tumor recurrence. J Magn Reson Imaging 49:719–730
11. Zhang L, Chen J, Jiang H et al (2022) MR elastography as a biomarker for prediction of early and late recurrence in HBV-related hepatocellular carcinoma patients before hepatectomy. Eur J Radiol 152:110340
12. Dong Y, Zheng Q, Wang Z et al (2019) Higher matrix stiffness as an independent initiator triggers epithelial-mesenchymal transition and facilitates HCC metastasis. J Hematol Oncol 12:112
13. Cho HJ, Kim B, Kim HJ et al (2020) Liver stiffness measured by MR elastography is a predictor of early HCC recurrence after treatment. Eur Radiol 30:4182–4192
14. Jung KS, Kim SU, Choi GH et al (2012) Prediction of recurrence after curative resection of hepatocellular carcinoma using liver stiffness measurement (FibroScan®). Ann Surg Oncol 19:4278–4286
15. Lee PC, Chiou YY, Chiu NC et al (2020) Liver stiffness measured by acoustic radiation force impulse elastography predicted prognoses of hepatocellular carcinoma after radiofrequency ablation. Sci Rep 10:2006
16. Lee YR, Park SY, Kim SU et al (2017) Using transient elastography to predict hepatocellular carcinoma recurrence after radiofrequency ablation. J Gastroenterol Hepatol 32:1079–1086
17. Jung KS, Kim JH, Kim SU et al (2014) Liver stiffness value-based risk estimation of late recurrence after curative resection of hepatocellular carcinoma: development and validation of a predictive model. PLoS One 9:e99167
18. Affo S, Yu LX, Schwabe RF (2017) The role of cancer-associated fibroblasts and fibrosis in liver cancer. Annu Rev Pathol 12:153–186
19. Kim MN, Kim SU, Kim BK et al (2015) Increased risk of hepatocellular carcinoma in chronic hepatitis B patients with transient elastography-defined subclinical cirrhosis. Hepatology 61:1851–1859
20. Akima T, Tamano M, Hiraishi H (2011) Liver stiffness measured by transient elastography is a predictor of hepatocellular carcinoma development in viral hepatitis. Hepatol Res 41:965–970
21. Dietrich CF, Bamber J, Berzigotti A et al (2017) EFSUMB guidelines and recommendations on the clinical use of liver ultrasound elastography, update 2017 (Long Version). Ultraschall Med 38:e48
22. Gao Y, Zheng J, Liang P et al (2018) Liver fibrosis with two-dimensional US shear-wave elastography in participants with chronic hepatitis B: a prospective multicenter study. Radiology 289:407–415
23. Gu JH, Zhu L, Jiang TA (2021) Quantitative ultrasound elastography methods in focal liver lesions including hepatocellular carcinoma: from diagnosis to prognosis. Ultrasound Q 37:90–96
24. Yao Z, Dong Y, Wu G et al (2018) Preoperative diagnosis and prediction of hepatocellular carcinoma: radiomics analysis based on multi-modal ultrasound images. BMC Cancer 18:1089
25. Praktiknjo M, Krabbe V, Pohlmann A et al (2018) Evolution of nodule stiffness might predict response to local ablative therapy: a series of patients with hepatocellular carcinoma. PLoS One 13:e0192897
26. Park HS, Kim YJ, Yu MH, Jung SI, Jeon HJ (2015) Shear wave elastography of focal liver lesion: intraobserver reproducibility and elasticity characterization. Ultrasound Q 31:262–271

27. Zhong X, Chen L, Long H et al (2022) The "stiff rim" sign of hepatocellular carcinoma on shear wave elastography: correlation with pathological features and potential prognostic value. Abdom Radiol (NY). https://doi.org/10.1007/s00261-022-03628-9
28. Guibal A, Boularan C, Bruce M et al (2013) Evaluation of shearwave elastography for the characterisation of focal liver lesions on ultrasound. Eur Radiol 23:1138–1149
29. Grgurevic I, Bokun T, Salkic NN et al (2018) Liver elastography malignancy prediction score for noninvasive characterization of focal liver lesions. Liver Int 38:1055–1063
30. Tian WS, Lin MX, Zhou LY et al (2016) Maximum value measured by 2-D shear wave elastography helps in differentiating malignancy from benign focal liver lesions. Ultrasound Med Biol 42:2156–2166
31. Lee S, Jung Y, Bae Y (2016) Clinical application of a color map pattern on shear-wave elastography for invasive breast cancer. Surg Oncol 25:44–48
32. Evans A, Whelehan P, Thomson K et al (2012) Invasive breast cancer: relationship between shear-wave elastographic findings and histologic prognostic factors. Radiology 263:673–677
33. Cong WM, Bu H, Chen J et al (2016) Practice guidelines for the pathological diagnosis of primary liver cancer: 2015 update. World J Gastroenterol 22:9279–9287
34. Desmet VJ, Gerber M, Hoofnagle JH, Manns M, Scheuer PJ (1994) Classification of chronic hepatitis: diagnosis, grading and staging. Hepatology 19:1513–1520
35. Budczies J, Klauschen F, Sinn BV et al (2012) Cutoff Finder: a comprehensive and straightforward web application enabling rapid biomarker cutoff optimization. PLoS One 7:e51862
36. Riegler J, Labyed Y, Rosenzweig S et al (2018) Tumor elastography and its association with collagen and the tumor microenvironment. Clin Cancer Res 24:4455–4467
37. Mohammadi H, Sahai E (2018) Mechanisms and impact of altered tumour mechanics. Nat Cell Biol 20:766–774
38. Piersma B, Hayward MK, Weaver VM (2020) Fibrosis and cancer: a strained relationship. Biochim Biophys Acta Rev Cancer 1873:188356
39. Zhong X, Peng J, Xie Y et al (2022) A nomogram based on multi-modal ultrasound for prediction of microvascular invasion and recurrence of hepatocellular carcinoma. Eur J Radiol 151:110281
40. Li M, Yin Z, Hu B et al (2022) MR elastography-based shear strain mapping for assessment of microvascular invasion in hepatocellular carcinoma. Eur Radiol 32:5024–5032
41. Kubo N, Araki K, Kuwano H, Shirabe K (2016) Cancer-associated fibroblasts in hepatocellular carcinoma. World J Gastroenterol 22:6841–6850
42. Hoshida Y, Villanueva A, Kobayashi M et al (2008) Gene expression in fixed tissues and outcome in hepatocellular carcinoma. N Engl J Med 359:1995–2004
43. O'Rourke JM, Sagar VM, Shah T, Shetty S (2018) Carcinogenesis on the background of liver fibrosis: implications for the management of hepatocellular cancer. World J Gastroenterol 24:4436–4447
44. Feng JC, Li J, Wu XW, Peng XY (2016) Diagnostic accuracy of supersonic shear imaging for staging of liver fibrosis: a meta-analysis. J Ultrasound Med 35:329–339
45. Ju MJ, Qiu SJ, Fan J et al (2009) Peritumoral activated hepatic stellate cells predict poor clinical outcome in hepatocellular carcinoma after curative resection. Am J Clin Pathol 131:498–510
46. Wallace MC, Friedman SL (2014) Hepatic fibrosis and the microenvironment: fertile soil for hepatocellular carcinoma development. Gene Expr 16:77–84
47. Ferraioli G, Tinelli C, Zicchetti M et al (2012) Reproducibility of real-time shear wave elastography in the evaluation of liver elasticity. Eur J Radiol 81:3102–3106


## Publisher's Note